NASA Contractor Report 170394

WIND TUNNEL TESTS OF A FREE-WING/ FREE-TRIMMER MODEL

Doral R. Sandlin

Grant NSG 4020
December 1982

NASA

NASA Contractor Report 170394

WIND TUNNEL TEST OF A FREE-WING/ FREE-TRIMMER MODEL

Doral R. Sandlin
Aeronautical and Mechanical Engineering Department
California Polytechnic State University
San Luis Obispo, California

Prepared for
Ames Research Center
Dryden Flight Research Facility
under Grant NSG 4020

National Aeronautics and
Space Administration
1982

WIND TUNNEL TESTS OF A FREE-WING/ FREE-TRIMMER MODEL

Grant No. NSG 4020

Submitted to:

The National Aeronautics and Space Administration

By

Dr. Doral R. Sandlin, Professor

Aeronautical and Mechanical Engineering Department
California Polytechnic State University
San Luis Obispo, CA 93407

May 1981

TABLE OF CONTENTS

LIST OF TABLES

LIST OF FIGURES

INTRODUCTION

General aviation aircraft with low wing loading are known to be very responsive to the gust conditions encountered in turbulent air. Gust responsiveness causes poor riding qualities which is a factor in limiting the widespread acceptance of general aviation aircraft as a mode of transportation. Riding qualities can be improved by increasing wing loading. However, an increase of wing loading increases minimum flying speed which is the speed used in landing. Aircraft safety considerations make it undesirable to increase landing speed.

Another very effective method of gust alleviation exists. The aircraft configuration used for this method consists of a wing which is free to pivot about a spanwise axis. The pivot axis is located forward of the aerodynamic center as shown in Figure 1(a). Balancing moments needed to achieve equilibrium are generated by deflecting the trailing-edge surface, which can be controlled by the pilot. The pilot can select the trim angle of attack by positioning this control. Gust alleviation is achieved by decoupling the wing from the aircraft. The pitching moment of inertia is much less for the wing than for the entire aircraft and the rate of gust alleviation increases as pitching moment of inertia decreases. A significant reduction in turbulence response is the result.

This configuration has been termed the free-wing aircraft. The concept was patented by Daniel Zuck in 1944. Several analytical and wind tunnel studies of this configuration have been made (see Ref. 3, 4, and Ref. 5). From these studies it has been concluded that about a 54% reduction in the RMS load factor can be realized.

The major shortcoming of the free-wing configuration is that only relatively low maximum lift coefficients are obtainable. High values of lift coefficient are usually achieved by using flaps placed on the trailing edge of the wing. Flaps on the free-wing create negative (leading edge down) pitching moments and utilize area needed by control tabs to trimout moments.

The Dryden Flight Research Center of NASA has conceived of an extension of the free-wing to include a separate trimmer surface located either in a canard arrangement forward of the wing or located after and at the tips of the wing (see Figures 2 and 3). This arrangement provides sufficient trimming power to permit the use of high-lift trailing edge flaps on the free wing. This configuration has been termed the free-wing/free-trimmer aircraft since both surfaces are free to rotate about a spanwise axis. (See Figure 1(b)).

The dynamics of both the forward and after free-wing/free-trimmer configurations have been analytically evaluated by Battelle Columbus Laboratories under contract to NASA. One study investigated the longitudinal stick-fixed modes of motion for these configurations and the maximum trimmed lift coefficients obtainable. Another study investigated the lateral-directional behavior. The longitudinal behavior of the aircraft was analyzed by constructing a mathematical model which consisted of 13 simultaneous homogenous equations, with 13

variables. Unsteady aerodynamic effects for both lifting surfaces were included (see Ref. 4). This complex set of equations was used to assess the response to symmetric vertical turbulence. The conclusions of the study were:

1. For the trimmer area ratio considered (1/6), the most promising configuration employs wingtip-mounted trimming surfaces placed aft of the wing hinge line with a moment arm of one wing chord length. Of the configurations examined in this study, this arrangement alone could provide excellent alleviation of vertical gust loads while exceeding the maximum lift capability of pure free-wing configurations, and while meeting fundamental criteria for the stability of the stick-fixed longitudinal modes.

2. For vertical gust alleviation, forward trimmers are inferior to aft-mounted surfaces because of adverse wing pitching moments caused by transient aerodynamic forces on the trimming surfaces.

3. Mass balancing of the trimmer surface about its hinge axis is vital for precluding adverse effects on the stability of the characteristic modes. In particular, aft imbalance must be avoided.

4. Longitudinal displacement of the center of gravity of the fuselage assembly appears to be more significant for free-wing/free-trimmer configurations than for pure free-wing aircraft. Forward displacement decreases the damping of the phugoid mode while aft displacement decreases the damping of one of the short-period modes. The effect of fuselage imbalance is more pronounced for slow-speed flight, and the sensitivity depends upon the aerodynamic design of the fuselage assembly.

5. Small variations in the wing assembly center of gravity (of the order of a few percent of wing chord) have no significant effect on the in-flight characteristic modes, but center of gravity locations aft of the wing hinge axis should be avoided to facilitate smooth landings.

6. Forward-trimmer configurations are more efficient from a weight standpoint than aft trimmers, and could, if properly sized and placed, provide a lighter total wing weight than a pure free-wing. The aft-trimmer configuration incurs a higher weight penalty because of the additional counterweight needed to balance the wing assembly about its hinge axis.

No wind tunnel test of the configuration analysed by Battelle has been conducted.

The purpose of this study is to perform wind tunnel tests to determine the dynamic behavior of a free-wing/free-trimmer model. Battelle has provided the results of the computer algorithm of the equations of motion of the free-wing/free trimmer with the wind tunnel model parameters as inputs. A comparison of the results of the wind tunnel test and the computer analysis has been made in order to evaluate the validity of the math model.

Scope

The investigation described in this report is limited to the control-fixed longitudinal motion of a free-wing/free-trimmer system which included only the wing and the trimmer. The wing is pivoted at the 5% chord position. The trimmer was mounted aft of the wing

pivot on the wing tip at a distance of one wing chord from the wing pivot to the trimmer pivot.

The trimmer was also confined to longitudinal motion only. The pivot location of the trimmer was at the 13% trimmer chord position. The flap size was 20% of the trimmer chord. Two orientations of the trimmer, one with the camber the same as the wing camber and one with the cambers opposite, were tested. Tests were made with the trimmer both fixed and free to rotate.

The wing/trimmer system was mounted vertically on a bearing in the tunnel to eliminate gravitational influences and provide a response more indicative of the aerodynamic moments associated with the configuration.

MODEL DESCRIPTION

The model of the wing and trimmer was constructed of solid aluminum with a chord of 6-15/16 and a span of 21-1/4 inches giving an aspect ratio of 3.01 for the wing. An end plate was attached to one end of the wing creating a semi-span model of the wing with an effective aspect ratio of 6.12. The trimmer chord length was 4 and the span was 6 inches, giving an aspect ratio of 1.5. The maximum thickness of both the wing and trimmer was 12% of the chord and the airfoil section used for both was a NASA 23012 section.

The aft location of the trimmer was selected since it was the most promising location of the trimmer as determined in the analytical study (Ref. 4). The ratio of the trimmer area to wing area was 1 to 6.14 and the ratio of their respective aspect ratio was 1 to 4.08. The trimmer was mounted to a wing tip attachment plate by a 8" shaft

with a supporting bearing in the plate. Mass balancing was achieved with a boom and a position variable lead weight mounted on the left trimmer tip. The wing was mass balanced with a position variable weight and a rod attached to the wing pivot axis. The wing mass balance was under the wind tunnel test section floor and was not exposed to the flow within the tunnel. A drawing of the model of the wing and trimmer is given in Figure 4 . A picture of the unassembled wing, trimmer and end plate is given in Figure 5 . Table 1 gives the weights of the components of the system.

MOUNTING SYSTEM DESCRIPTION

The wing and trimmer were mounted with the pivot axis of the wing perpendicular to the floor of the tunnel. The pivot axis or support shaft of the wing extended through the wind tunnel floor and was isolated from tunnel vibrations. The shaft in turn was supported by a large air bearing which provided a frictionless pivot system. Figure 6 shows a drawing of the air bearing, supporting shaft and end plate. Air supply to the bearing was routed through a pressure regulator and an electrical monitor system was connected to insure that the bearing was friction free.

The end plate was mounted inside the tunnel and approximately four inches from the floor to insure that the model was outside of the test section boundary layer. The wing was mounted above the end plate. A small pole was mounted to the end of the wing opposite the end plate and a three-wire, Y-brased system was attached in order to make the model more rigid. A picture of the system assembled and resting on the air bearing is shown in Figure 7.

INSTRUMENTATION

Two potentiometers were used to record the positions of the wing and trimmer as functions of time. One potentiometer was mounted on the trailing edge of the wing as shown in Figure 4. The brush of the potentiometer was connected to the pivoting support shaft of the trimmer. The shaft extended into the resistance ring and the brush made contact with the ring. Friction between the brush and ring was kept to a minimum necessary for good electrical contact. The electrical leads to the potentiometer were stored in a groove machined in the trailing edge of the wing as shown in Figure 5. The groove and wiring were covered with fiberglass and sanded smooth so as not to disturb the flow.

Another potentiometer was attached in a similar fashion to the support shaft of the wing which pivots with the wing. The two potentiometers were connected to an X-Y Plotter. As the wing is displaced through positive and negative angles of attack, the supporting pivot axis of the wing and trimmer rotates. The angular displacement of the shafts causes voltage outputs of the potentiometer to vary. The variations of the output voltages were recorded on an X-Y Plotter which had a known sweep rate. Since the output voltages were directly related to wing position, a plot of wing angle of attack and trimmer displacement angle (angle between cords of wing and trimmer) as functions of time were obtained from the X-Y Plotter. Figure 8 is a picture of the Plotter used.

A different data recording system was used for several tests with the wing fixed and the trimmer free to rotate. A compass card was taped to the wing and a pointer to the trailing edge of the trimmer. A digital timer was placed in the field of view and a video camera was

used to record trimmer position indicated by the pointer superimposed on the compass card. The corresponding time was indicated by the digital timer.

WIND TUNNEL

Two different wind tunnels were used. The variable low speed recirculating wind tunnel at the United States Naval Academy at Annapolis, Maryland, was used to collect most of the data. This tunnel has a 3 X 4 feet test section and a flow velocity range up to 200 mph. In addition, the variable speed draw through wind tunnel at Cal Poly was used for the fixed wing tests. This tunnel has a 3 X 4 feet test section and a flow velocity range up to 125 mph.

MOMENT OF INERTIA DETERMINATION

In order to measure the moment of inertia of the model, a torsion pendulum was constructed and instrumented. The object of unknown moment of inertia is attached to a stiff wire which is supported at one end. A light reflecting strip is attached to the object. The object is disturbed from equilibrium by twisting to a small angle and released. A lamp beams light at the reflecting strip and the reflected light is directed through a lens into a photo transistor. An electric pulse is generated for each oscillation of the object. The pulses are amplified by a DC amplifier and directed to a strip chart recorder where they are recorded as functions of time. The period of oscillation which is a function of the moment of inertia of the object is determined from the recorded data.

Several objects of known moments of inertia were used and the oscillation periods determined. Two calibration curves of moment of inertia vs. period were constructed and are shown in Figures 9 and 10.

Figure 10 is for the trimmer and Figure 9 is for the complete model. The trimmer and complete model were mounted on the torsional pendulum and disturbed. Figure 11 shows the trimmer being tested. The periods were recorded and used with the calibration curves to determine the moments of inertia. Values obtained were .001072 slugs-ft^2 for the trimmer and .095033 slugs-ft^2 for the entire assembly (wing + trimmer + balance weights + air bearing).

TEST PROCEDURE

The model was mounted vertically in the wind tunnel and the wing and trimmer potentiometer were connected to separate needles on the X-Y Plotter. A compass card on the floor on the tunnel was used to determine the angle of attack of the wing. Angles of attack as indicated on the compass were calibrated with those indicated on the X-Y Plotter. The trimmer potentiometer measured the angle between the chords of the wing and trimmer. The chords of the two surfaces were aligned and the zero angles were marked on the graph paper of the X-Y Plotter.

After the wind tunnel was started and set to the desired speed, the model was disturbed from equilibrium by displacing the wing to a large angle of attack and releasing. The oscillation of the wing and trimmer were recorded on the X-Y Plotter. The wing angle of attack and the angles between the wing and trimmer chords were recorded as functions of time. Wing disturbance or displacement angles of 5, 10 and 15 degrees above and 5, 10 and 15 degrees below the equilibrium angle of attack were used. Wind tunnel speeds of 75, 100 and 125 feet per second were used. Trimmer tab positions angle of 0,5, 7.5 and 10 degrees were tested. Tests were made with the camber of

the wing and the trimmer oriented in the same direction and in opposite directions. Several tests were made with the trimmer at various fixed angles between the wing and trimmer. Also, tests were made with an end plate attached to the wing between the wing and trimmer.

For tests with the wing fixed and the trimmer free to rotate, the tunnel speed was set at 75 feet per second. The trimmer tab position was set at 0 degrees and the camber of the wing was opposite to the camber of the trimmer. The trimmer was displaced to $\pm$ 20 degrees deflection angles and released. The oscillations of the trimmer were recorded with the video camera on magnetic tape.

The model parameters were provided to Battelle Research Laboratories to be used as inputs to their computer program of the math model of free-wing/free-trimmer system. (See Table 2 for model parameters provided as inputs to the computer program.) The programs predicted the roots of the characteristic equations of the system for several aerodynamic positions of the trimmer. These results are shown in Table 3.

DISCUSSION AND RESULTS

Comparison with Predicted Results

A flight speed of 75 ft/sec was used in obtaining the predicted results by Battelle. Two periodic and two aperiodic modes were obtained from the math model. The periodic modes correspond to the oscillator modes of the wing and trimmer. The trimmer model has a balance weight forward of its hinge axis (see Figure 7) that will cause a forward shift in the trimmer aerodynamic center location. Battelle provided computer predicted modes for several trimmer aerodynamic center locations (see Table 3).

In addition, Battelle provided computed time-histories of wing and trimmer angular rates to see if the mathematical model would predict the excitation of the second mode motion superimposed on the first mode. Figure 12 is the computed motion following in initial wing disturbance (an initial positive pitching rate of 0.1 radians/second). Figure 13 is a computed second case wherein the initial condition was a 0.1 radian/second rate applied to the trimmer, with the wing in initial equilibrium.

Table 4 shows the experimentally determined parameters for several pertinent test runs that were generated by disturbing the wing from equilibrium. If the values of p and q (the real and imaginary parts of the complex conjugate roots of the characteristic equation) for the trimmer are compared to those of the wing, it is apparent that for this initial condition, the trimmer motion follows the motion of the wing. The values of p and q are approximately the same for the wing and trimmer motion and compare very well with the computer predicted values. For run Number 2 with a test velocity of 75 fps and the tab setting of -7.5 degrees the values of p and q were $-.249 \pm i\ 5.71$ for the wing motion and the computed values were $-.2455 \pm i\ 5.721$. However, for run Number 8 with a test velocity of 75 fps and a tab setting of -5 degrees, the values of the roots were $-.460 \pm i\ 5.61$. The damping term p is higher than the computed value. The initial condition for the runs shown in Table 4 was a wing displacement from trim of ± 10 degrees. The trimmer was in an equilibrium position. These initial conditions did not always excite the second mode of motion. Figure 14 indicates that the second mode was only slightly excited but not excited at all for a similar run depicted in Figure 15. If the computed roots are correct, the time to half amplitude for the second mode is only .712 seconds as compared to 2.82 seconds for the first mode. Therefore, the second mode is not likely to be noticeable

very long unless it is heavily or repeatedly excited. In Figure 14 the mode 2 motion is apparently excited several times.

Although the computed plots of Figure 12 and 13 are time histories of angular rates and the experimental plot shown in Figure 14 is a time history of angular displacement, these graphs are similar. Both the computed and experimental graphs reveal the second oscillatory mode superimposed on the first mode. The alteration of the shape of the curve for motion of the first mode, caused by excitation of the second mode, is similar. Since the initial conditions were not the same, the excitation of the second mode occurs at different parts of the cycles. An attempt to extract the roots with any degree of accuracy of the second mode motion from the plotted data was not successful. The second mode was not sufficiently excited to obtain accurate results.

Since the roots of the first mode motion with the trimmer fixed were approximately the same as with the trimmer free, the roots of the second motion were determined with the wing fixed in an attempt to determine the approximate roots of the second mode. Eight different runs were made at a tunnel velocity of 75 fps, the wing fixed, the tab set at zero degrees and the initial conditions for four runs each of $\pm$20 degrees displacement. The values of p obtained for these initial conditions ranged from -.996 to -1.404 and values of q from 9.666 to 10.83 Computed values of p and q were -.9740 and 12.15.

Of course the flow fields for the system with both surfaces free is not exactly the same as with one surface fixed, and therefore the roots determined from their motion would not be expected to be exactly the same. Also, there was some friction present in the support bearing of the trimmer. Friction will increase the negative magnitude of p and decrease the magnitude of q.

Range of Equilibrium Angles of Attack

Tests were made at various trimmer tab angles in order to determine the range of equilibrium angles of attack (α_{eq}) attainable with a 20% chord tab. At 75 feet/sec tunnel speed and the camber of the two surfaces oriented in the same direction the maximum obtainable value of α_{eq} was two degrees. The tab setting for this condition was approximately six degrees. As expected, α_{eq} increased with tunnel velocity. For tab angles greater than six degrees,the trimmer stalls. In an attempt to prevent stall at such low values of tab settings, the boundary layer was tripped by placing a string near the leading edge. No significant improvement was observable. Since the trimmer operates at a negative α for surfaces with the same camber orientation and the stall α is lower for negative value of α, the camber of the trimmer was reversed in order to increase the stall α. With this configuration α_{eq} of five degrees was obtainable with maximum tab deflection angles of approximately 7.5 degrees.

With the tab set at approximately 10 degrees the trimmer was stalled, as indicated by the tufts on the trimmer surface and the motion of the wing trimmer. Figure 16 shows the trimmer stall condition. Leading edge slats could be used to increase the range of α_{eq}.

Effect of Velocity

Data was taken at tunnel velocities of 75, 100 and 125 ft/sec. Significant random errors were found to be present in the real parts of the roots. Since the real parts were determined from measured values of the amplitudes of the oscillations, the randomness was probbably caused by uncertainties in recording and measuring of amplitude values. Since the frequencies of the oscillation can be recorded and measured with greater precision, there should be less randomness

in the values of the imaginary parts of the roots. Although there was some randomness in the measured values of the q, there was less variation than in the values of the p. The values of q were found to be approximately directly proportional to tunnel velocity. There was too much randomness in the values of p to determine the effect of velocity.

Wing End Plates

An end plate was attached to the end of the wing between the wing and trimmer and data was recorded. Figure 15 shows data for the conditions of tunnel velocity of 75 ft/sec, tab setting of 7.5 degrees, and cambers opposite. The effect of the wind end plate was to reduce the strength of the wing vortex and decrease the operating angle between the wing and the trimmer. Neither the damping nor α_{eq} was affected appreciably.

Fixed Trimmer

Several tests were made with the trimmer fixed at a constant angle (β) between the chords of the trimmer and wing. β angles of 10, 20, 30, 35 and 40 degrees were used. The trimmer was observed to stall at a β of approximately 35 degrees.

The tests at various values of fixed β revealed that the damping is approximately constant for various values of β below trimmer stall, but the damping improves significantly when β is large enough so that the trimmer stalls. Apparently the large increase of drag due to stall improves the system damping. The values of the roots for a β of 20° and 40° are $-.167 \pm j7.90$ and $-.446 \pm j5.59$. A stalled free trimmer caused undamped motion of the system. Figures 16 and 17 show data for a stalled free and fixed trimmer.

A comparison was made of the data at a tunnel velocity of 75 ft/sec for free trimmer and fixed trimmer motion. The roots for free trimmer motion were -.249±j5.71 and the damping ratio was .0436. The values for fixed trimmer motion were -.167±j7.90 and -.0211. This data reveals that the damping is better for free trimmer configuration. This conclusion is in agreement with the results of the analytical study covered in Reference 4.

Data Repeatable

Four test runs were made to evaluate the repeatability of the data. Two runs were made with the trimmer free and two with the trimmer fixed. The data for the two free trimmer runs were overlayed on the same plot and is shown in Figure 19. The data for the fixed trimmer runs were overlayed and is shown in Figure 19. These plots show that the repeatability of the data was acceptable.

CONCLUSIONS

Wind tunnel tests of a free-wing/free-fixed trimmer model conducted in the Naval Academy's 3' x 4' wind tunnel and Cal Poly's 3' x 4' wind tunnel were performed for the purpose of checking the math model for the system. The following are the conclusions obtained from these tests:

1. The predicted values of the roots for an aerodynamic center located at the 25% chord matches very well with the experimentally determined roots for the wing.
2. While the roots of mode two motion are difficult to determine exactly, all experiment evidence indicates good agreement with computed values.
3. The equilibrium angles of attack that can be obtained with a 20% flap are limited to a maximum of approximately 5 degrees.

Some improvement was obtained by opposite orientation of the camber of the two surfaces.

4. The free trimmer will stall at tab deflections of 10 degrees, with opposite camber for the two surfaces.
5. Wing end plates decrease the operating angle between the wing and the trimmer, but do not appreciably affect damping or α_{eq}.
6. The values of q are approximately directly proportional to tunnel velocity. Randomness in values of p precluded conclusion concerning the effects of velocity.
7. Fixed trimmer stalls at β values of approximately 35 degrees and, while trimmer stall produces unfavorable dynamics for the free trimmer, it provides favorable dynamics for the fixed trimmer.
8. For the fixed trimmer damping stays nearly constant for all β angles up to stall and increases significantly when the trimmer stalls.
9. The free trimmer has better damping characteristics than the fixed trimmer.
10. The experimental data is repeatable for both the free and the fixed trimmer.

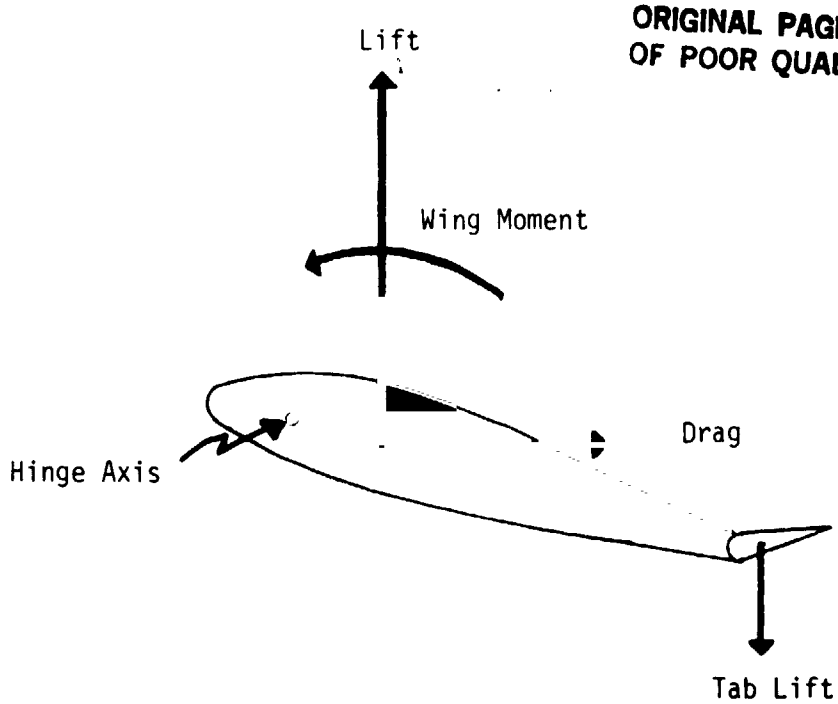

(a) Free Wing

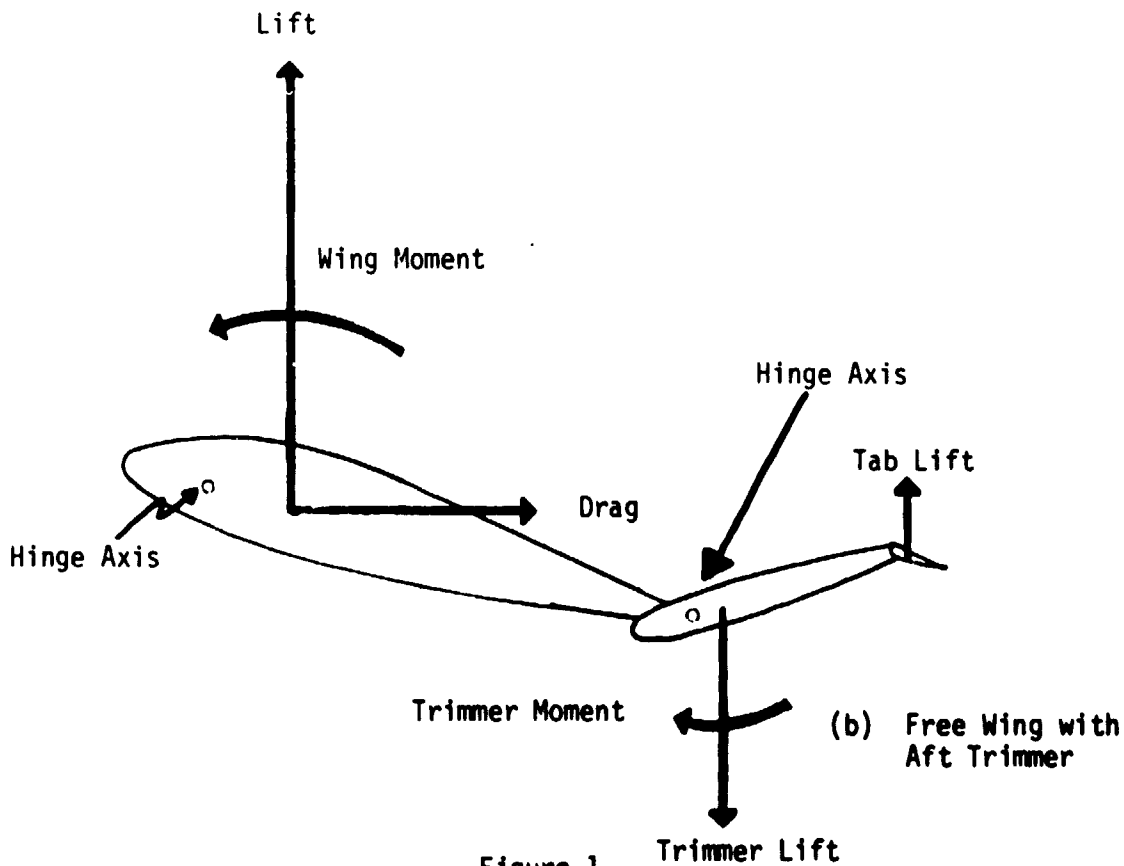

(b) Free Wing with Aft Trimmer

Figure 1

Cross Section Illustration

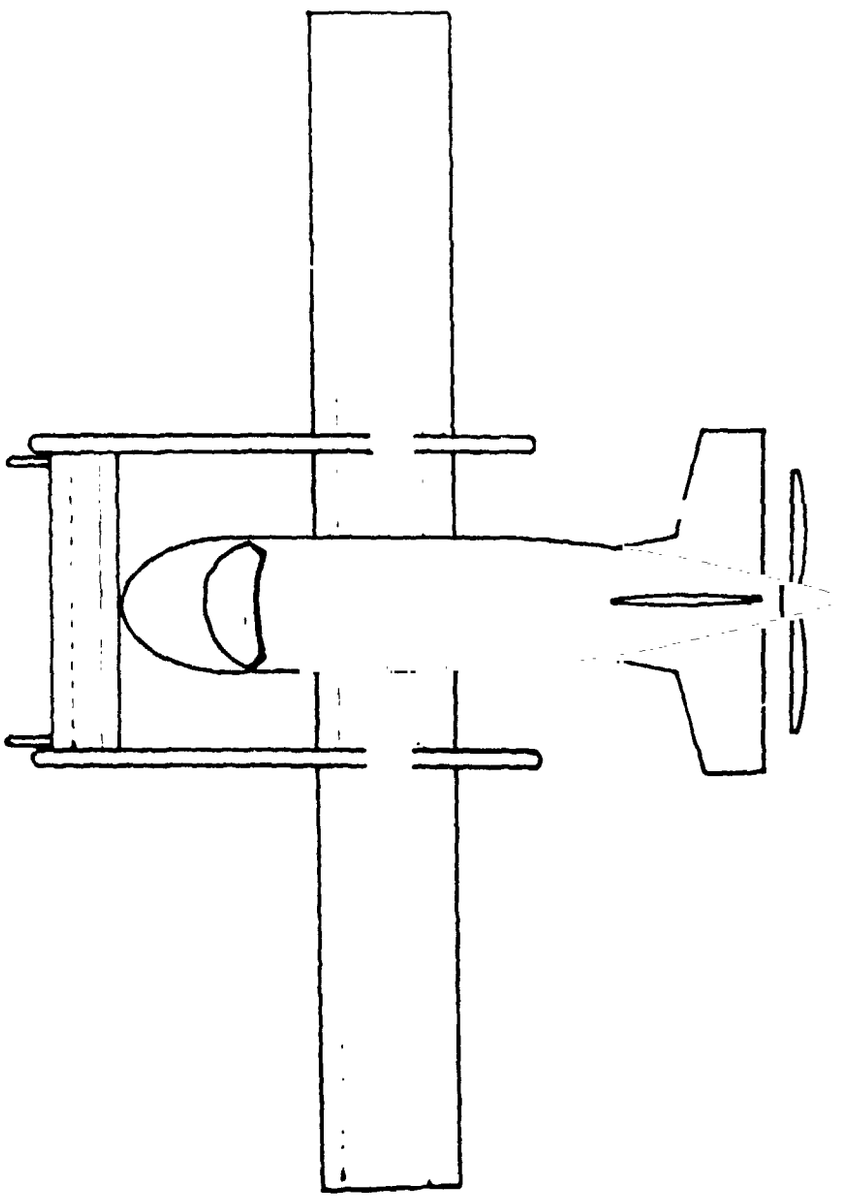

Figure 2

Aircraft With Free Wing/ Forward Free Trimmer

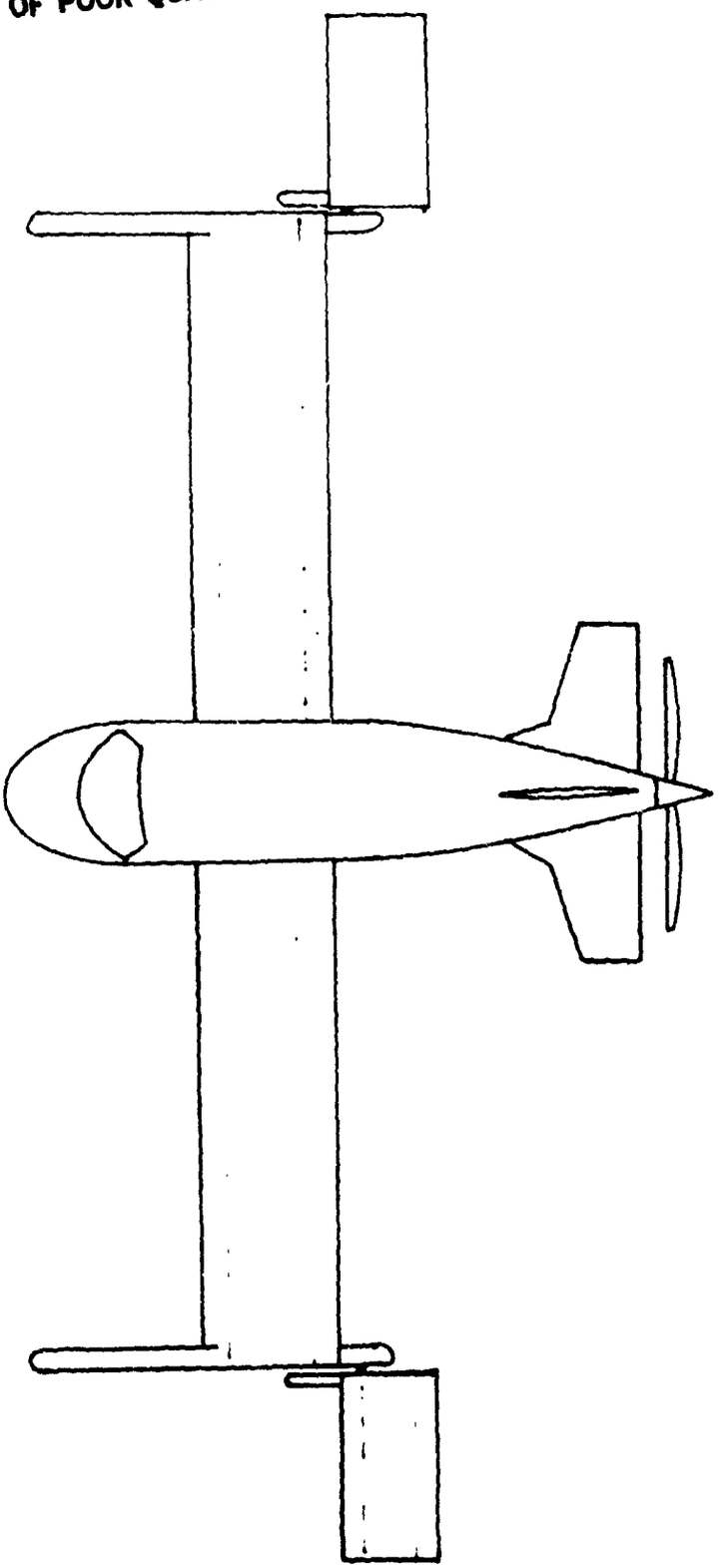

Figure 3

Aircraft with Free Wing/Aft Free Trimmer

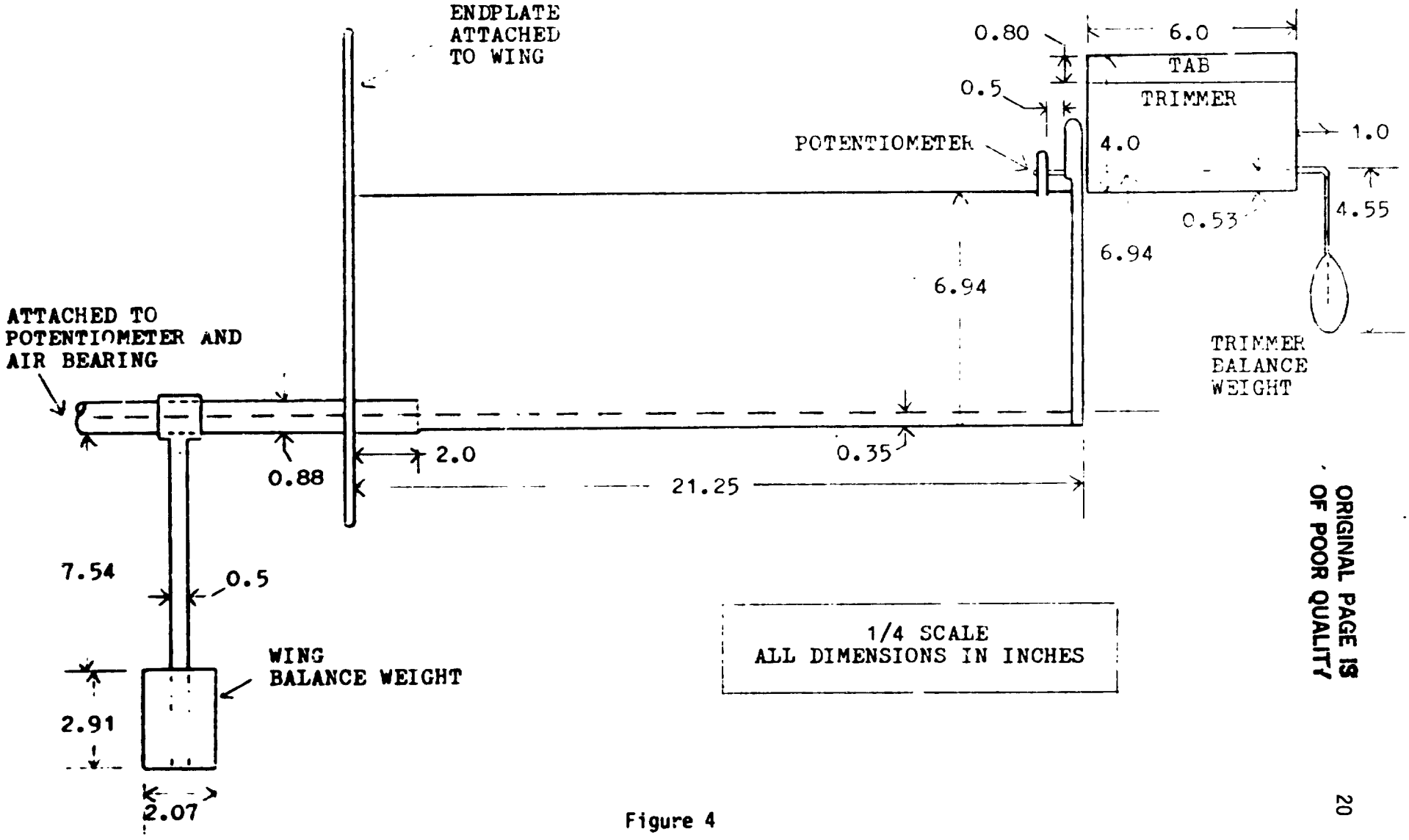

Figure 4

Free Wing/Free Trimmer Model

Figure 5

Model Components of Free Wing/Free Trimmer

Table 1

Weights

Wing Assembly (inc. endplate)	9 lbs. 6 oz.
Wing Counter Weight and Counter Wt. Arm	3 lbs. 15 oz.
Wing Root Axle	6 oz.
Trimmer	12 oz.
Trimmer Counter Wt.	5 oz.
Air Bearing	2 lbs. 15 oz.

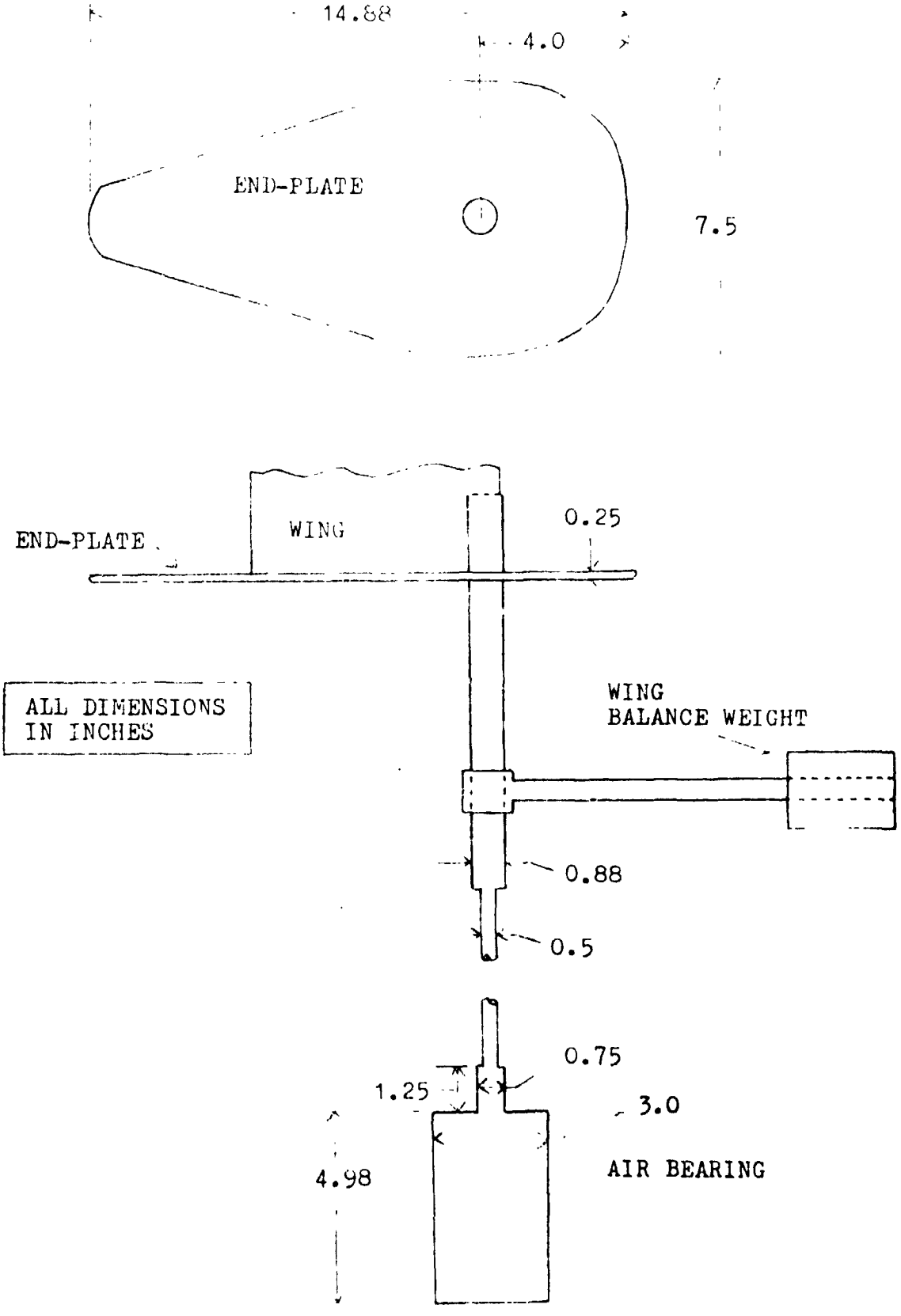

Figure 6

Model End-Plate, Wing Balance Weight and Air Bearing

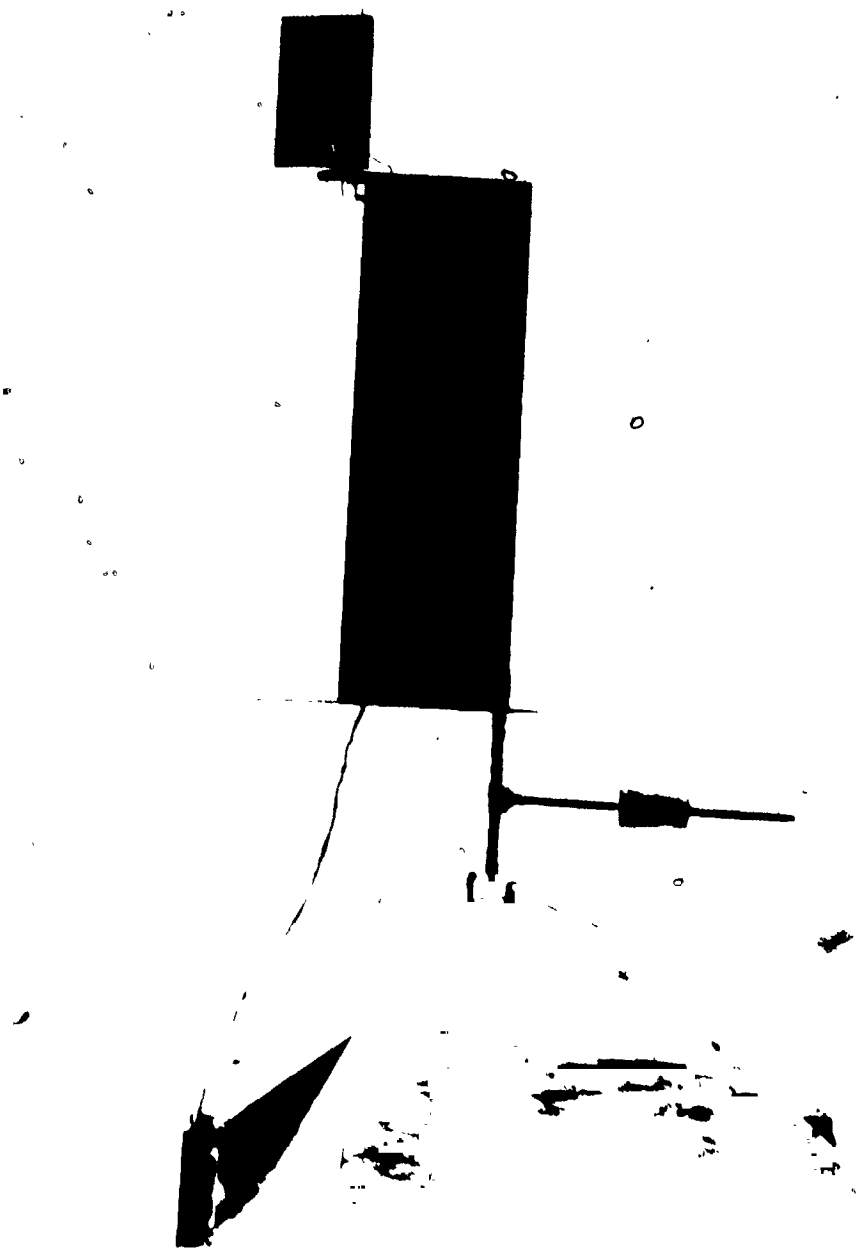

Figure 7

Assembled Model

Figure 8

Hewlett-Packard X-Y Plotter and Power Supply

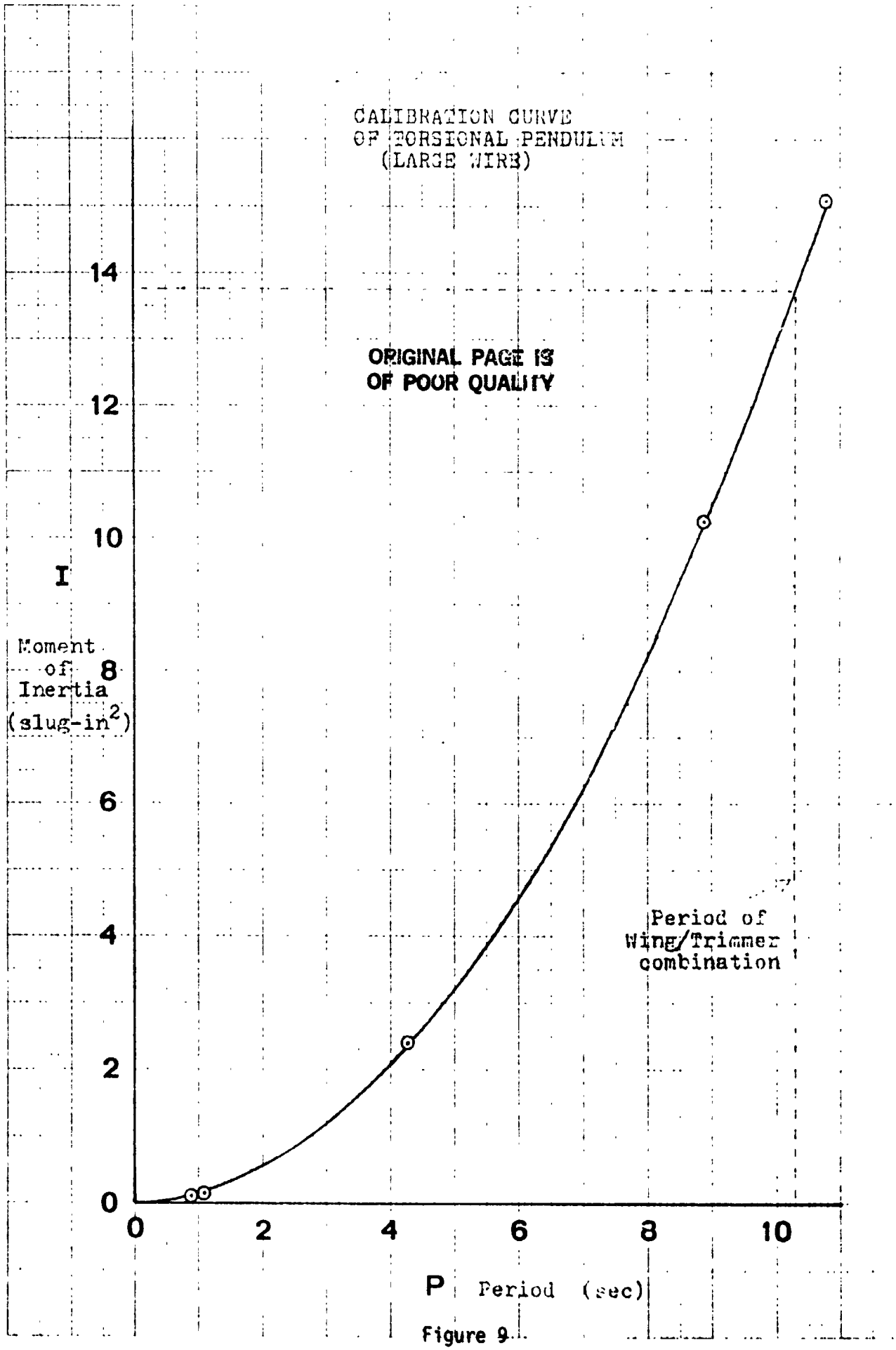

Figure 9

Calibration Curve of Torsional Pendulum (Large Wire)

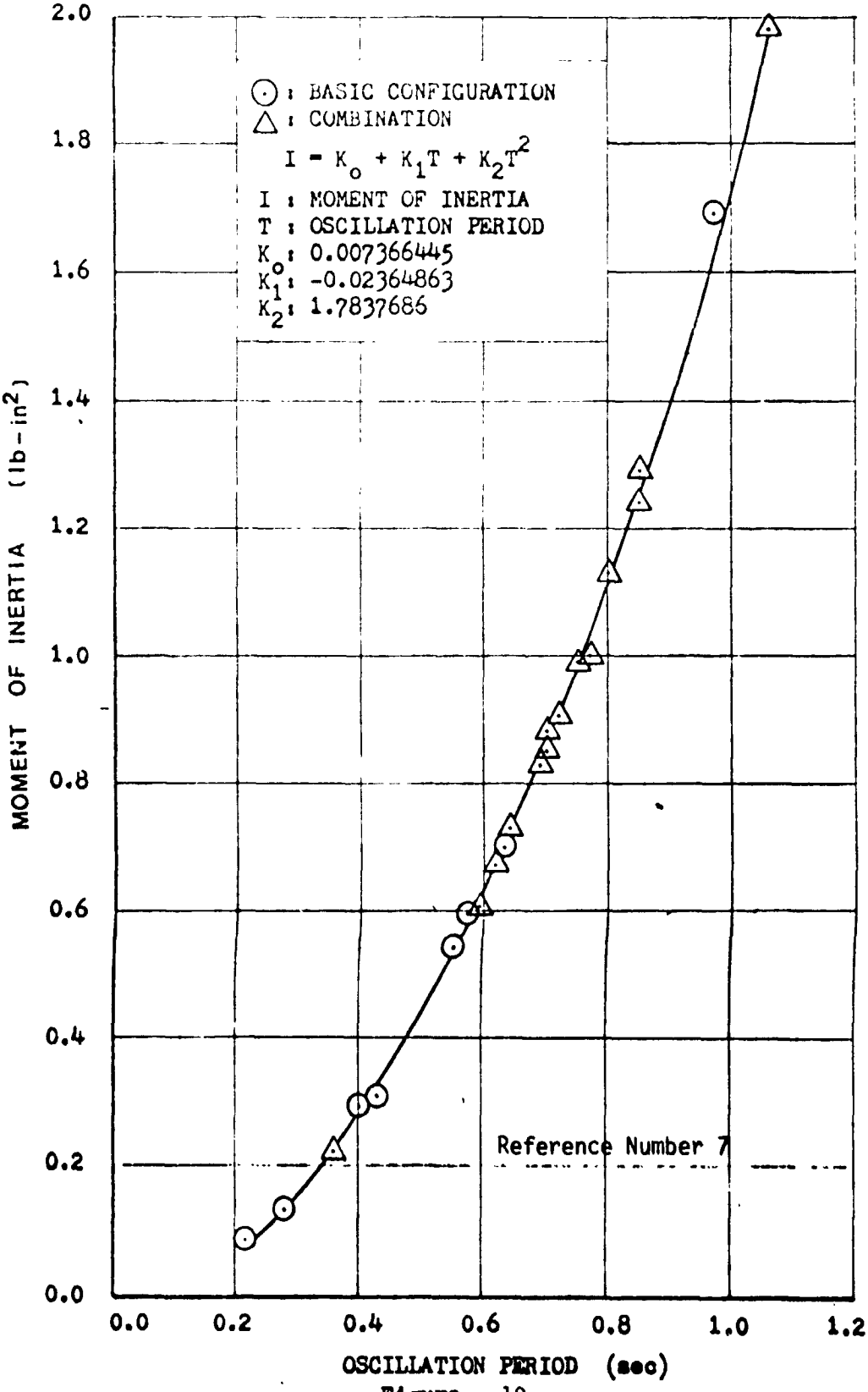

Figure 10

Figure 11

Test of Trimmer for Moment of Inertia

Table 2

Model Parameters Used as Input to Computer Program

(All areas, masses, and inertias were doubled to convert from the reflection-plane model to a complete configuration for program input purposes)

Wing Chord: .578125 ft.

Trimmer Chord: .3333 ft.

Wing Area: 2.0475 square ft.

Trimmer Area: .3333 square ft.

Distance from Wing Hinge to Wing Half-Chord: -.45 x Wing Chord

Distance from Wing Hinge to Trimmer Hinge: -1.0 x Wing Chord

Distance from Trimmer Hinge to Trimmer Half-Chord: -.37 x Trimmer Chord

Pitching moment of inertia of complete system: -0.19167 slugs-ft^2

(Wing, Wing Balance Weight, Trimmer, Trimmer Balance Weight, the Rotational Part of Air Bearing)

Pitching moment of inertia of Trimmer Assembly: -.00214 slugs-ft^2

Trimmer Assembly Mass: .066043 slugs

Atmospheric Density: .00237 slugs/cubic feet (assumed)

Table 3

Computed Roots of Wing/Trimmer Dynamic System

The computed roots for the 75 ft/sec tunnel speed are:

Oscillatory mode #1	$-.2455 \pm j\ 5.721$
Oscillatory mode #2	$-.9740 \pm j\ 12.15$
Aperiodic mode #1	-77.27
Aperiodic mode #2	-134.56

The roots are directly proportional to tunnel speed.

The nominal roots listed above are based on the assumption that the aerodynamic center of the trimmer assembly is at the quarter chord point. Since the attachment of the trimmer balance weight will cause some forward shift in the trimmer aerodynamic center location, the table below gives the locus of roots for the oscillatory modes as the trimmer aerodynamic center shifts forward. The aperiodic roots remain virtually unchanged.

U = 75 ft/sec

Trimmer a.c. location	Mode #1	Mode #2
$.25\bar{c}$	$-.2455 \pm j\ 5.721$	$-.9740 \pm j\ 12.15$
$.23\bar{c}$	$-.2476 \pm j\ 5.649$	$-.9255 \pm j\ 11.23$
$.21\bar{c}$	$-.2538 \pm j\ 5.533$	$-.8747 \pm j\ 10.26$
$.19\bar{c}$	$-.2721 \pm j\ 5.326$	$-.8138 \pm j\ 9.223$
$.17\bar{c}$	$-.3250 \pm j\ 4.893$	$-.7205 \pm j\ 8.192$
$.15\bar{c}$	$-.4364 \pm j\ 3.852$	$-.5705 \pm j\ 7.334$

Table 4

Experimental Results of Dynamic Wind Tunnel Tests of Wing/Trimmer Model

Run	Vel. (fps)	Tab (degrees)	Equil. (degrees)	WING MOTION p	WING MOTION q	WING MOTION x100	TRIMMER MOTION p	TRIMMER MOTION q	TRIMMER MOTION x100
1 *	75	- 7.5	4.0	-.241	5.85	-4.12	-.205	5.71	-3.59
2	75	- 7.5	4.8	-.249	5.71	-4.36	-.171	5.59	-3.06
3 *	75	-10				STALLED			
4	75	40	5.3	-.446	5.59	-7.99			
5	75	30	7.5	-.230	7.12	-3.23		TRIMMER FIXED	
6	75	20	4.0	-.167	7.90	-2.11			
7	75	10	2.0	-.187	7.98	2.34			
8	75	- 5	2.5	-.460	5.61	-8.20	-.490	5.64	-8.68
9	100	- 5	3.7	-.426	7.39	-5.76	-.391	7.99	-4.90
10	125	- 5	4.2	-.324	8.09	-4.01	-.411	8.77	-4.69
11 #	75	4	1.5	-.288	5.13	-5.62	-.283	5.19	-5.45

* with endplate
\# camber in same direction
All runs initially displaced 10 degrees from equilibrium.

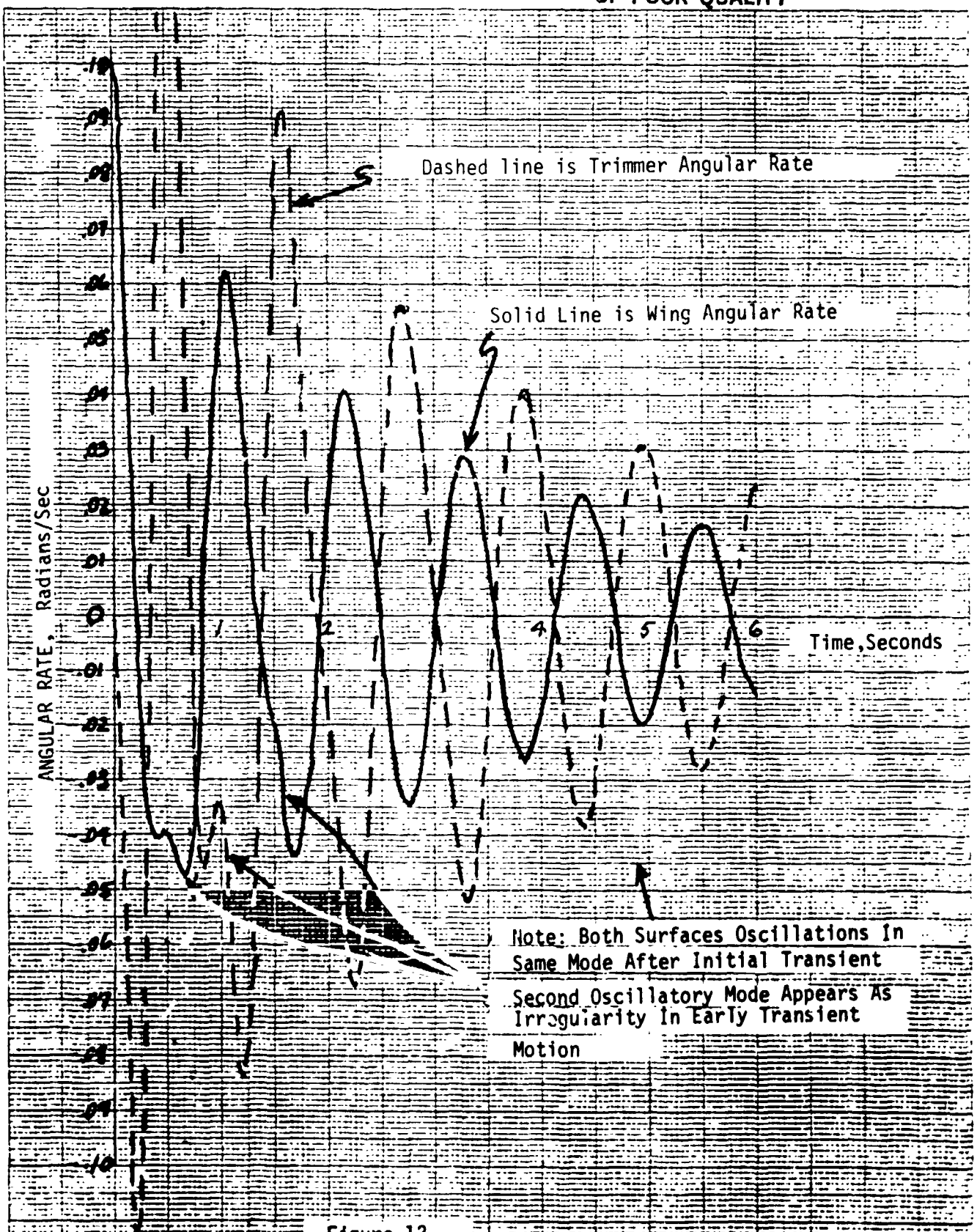

Figure 12

COMPUTED WING AND TRIMMER PITCHING RATE HISTORY

U = 75 ft/sec

Initial Condition: 0.1 Rad/sec Wing Angular Rate

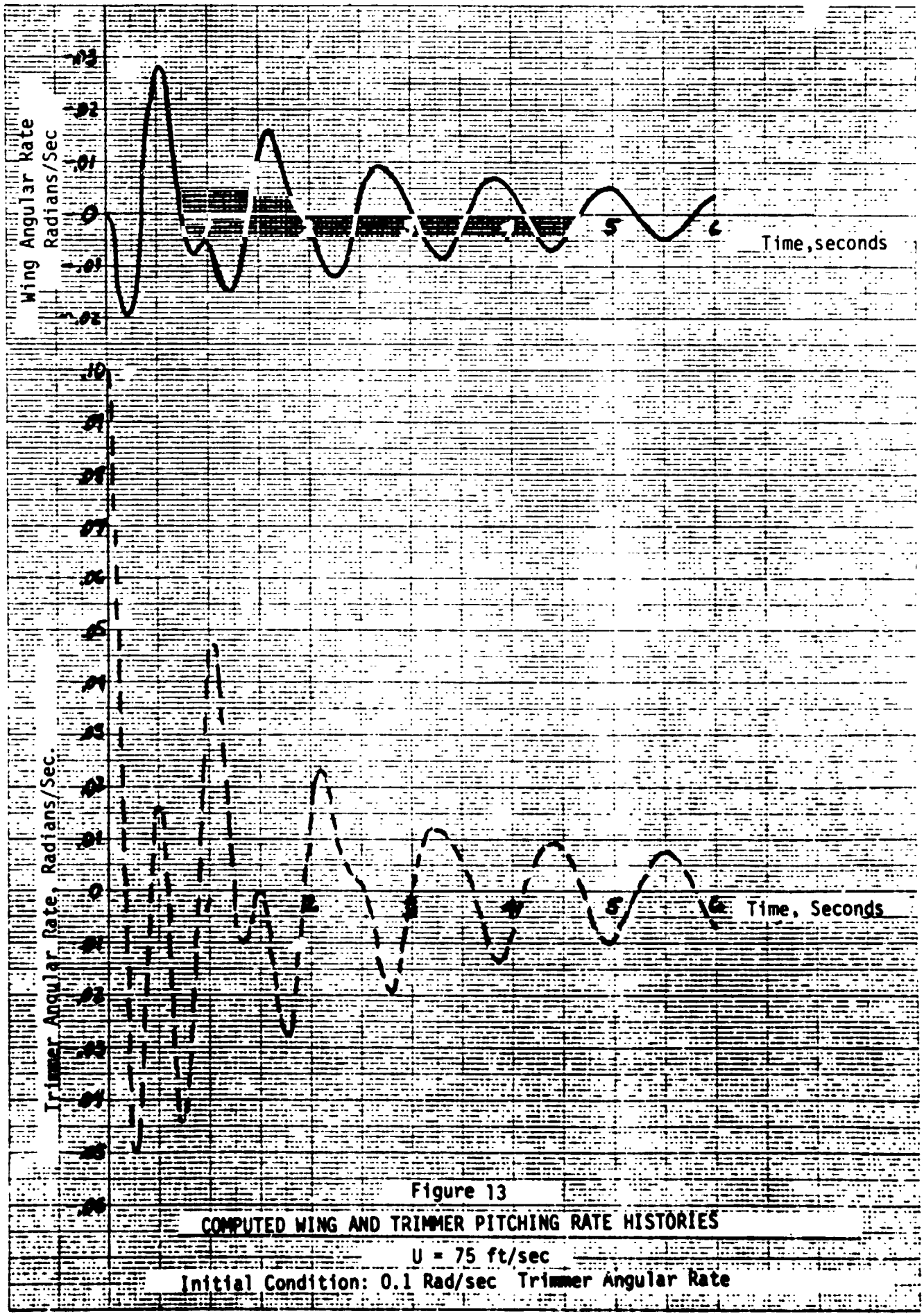

Figure 13

COMPUTED WING AND TRIMMER PITCHING RATE HISTORIES

U = 75 ft/sec

Initial Condition: 0.1 Rad/sec Trimmer Angular Rate

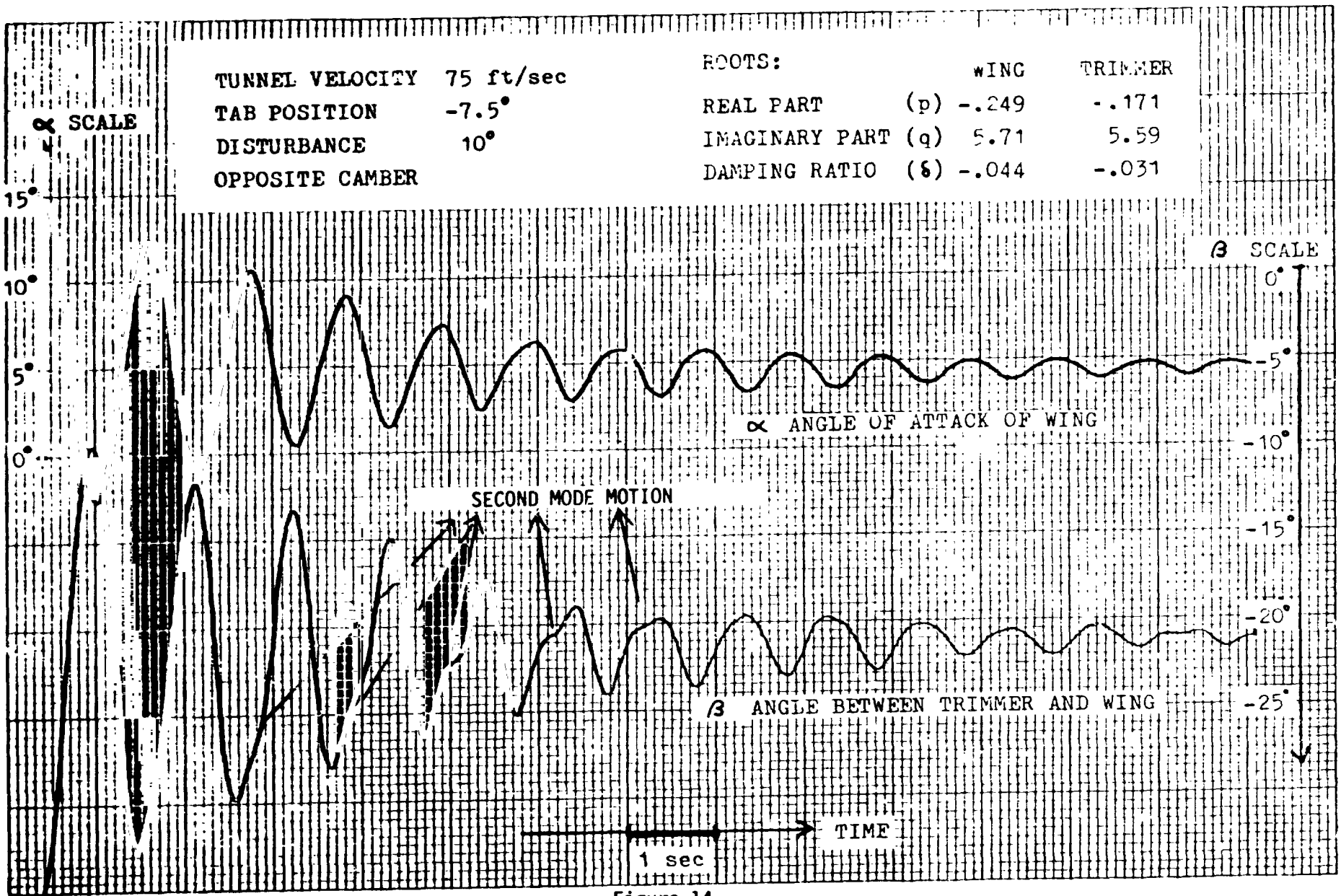

Figure 14

Time History of α and β with -7.5° Tab Position

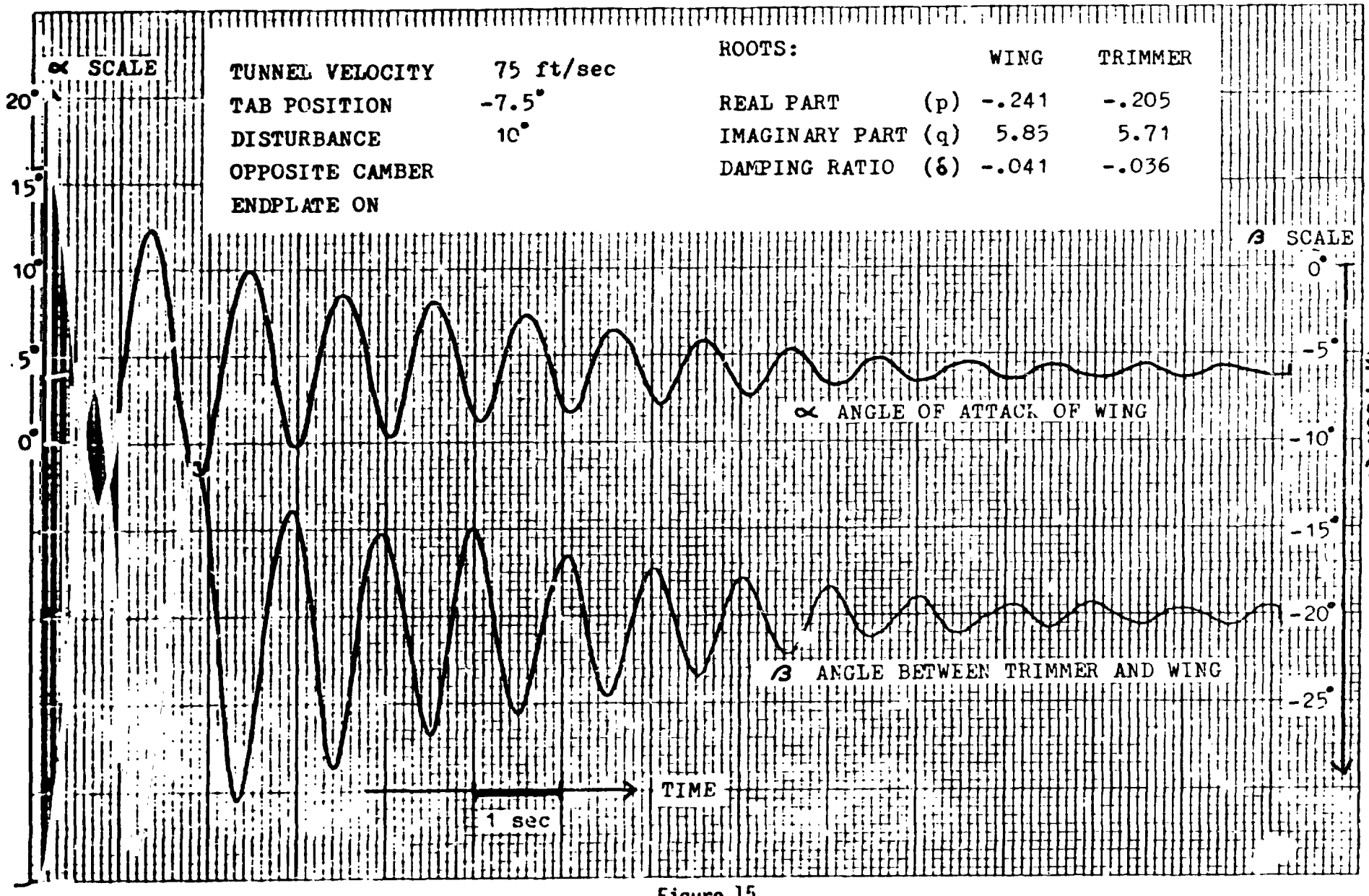

Figure 15

Time History of α and β with -7.5° Tab Position and End Plate Attached

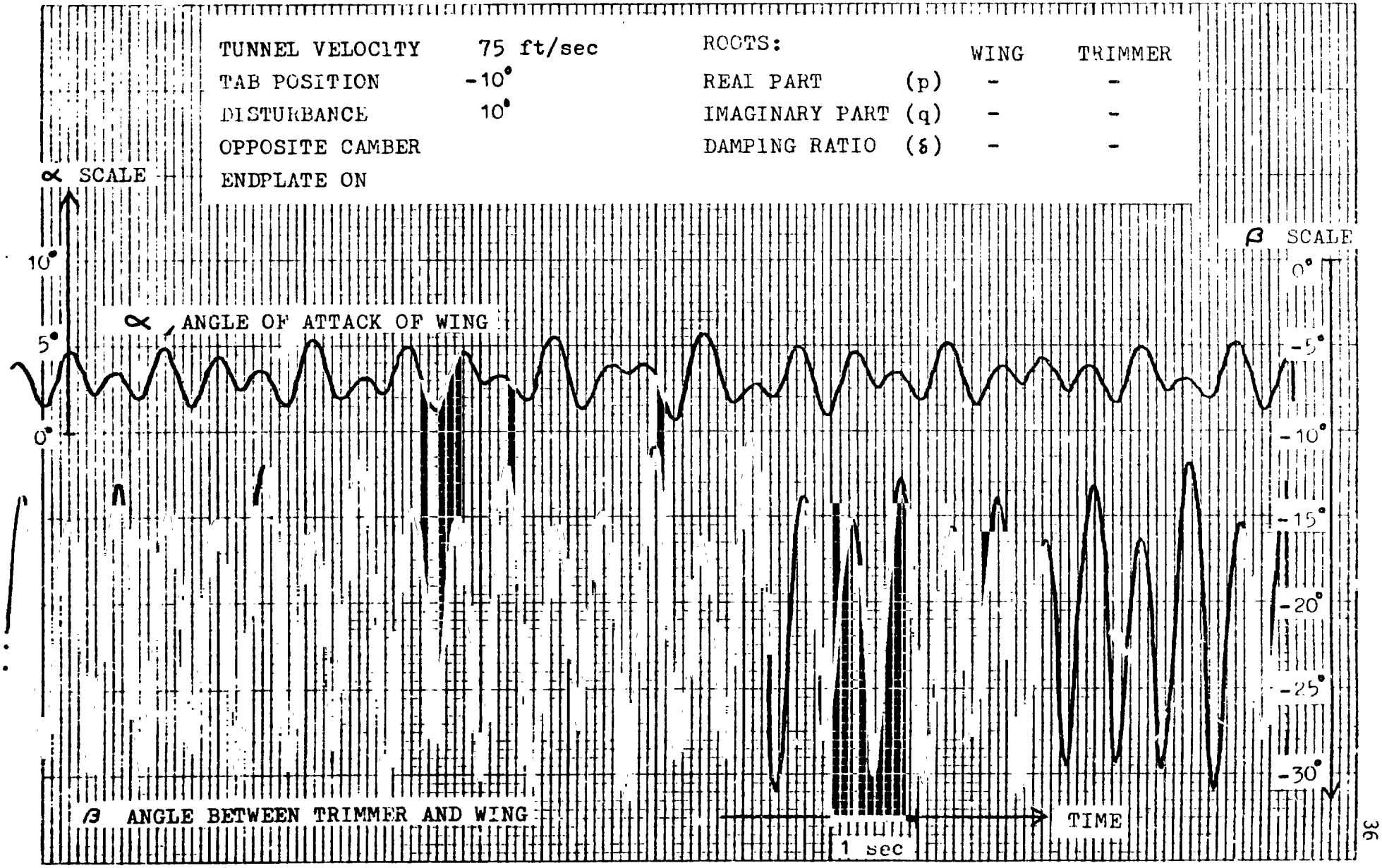

Figure 16

Time History of α and β with -10^{0} Tab Position (Trimmer Stalled)

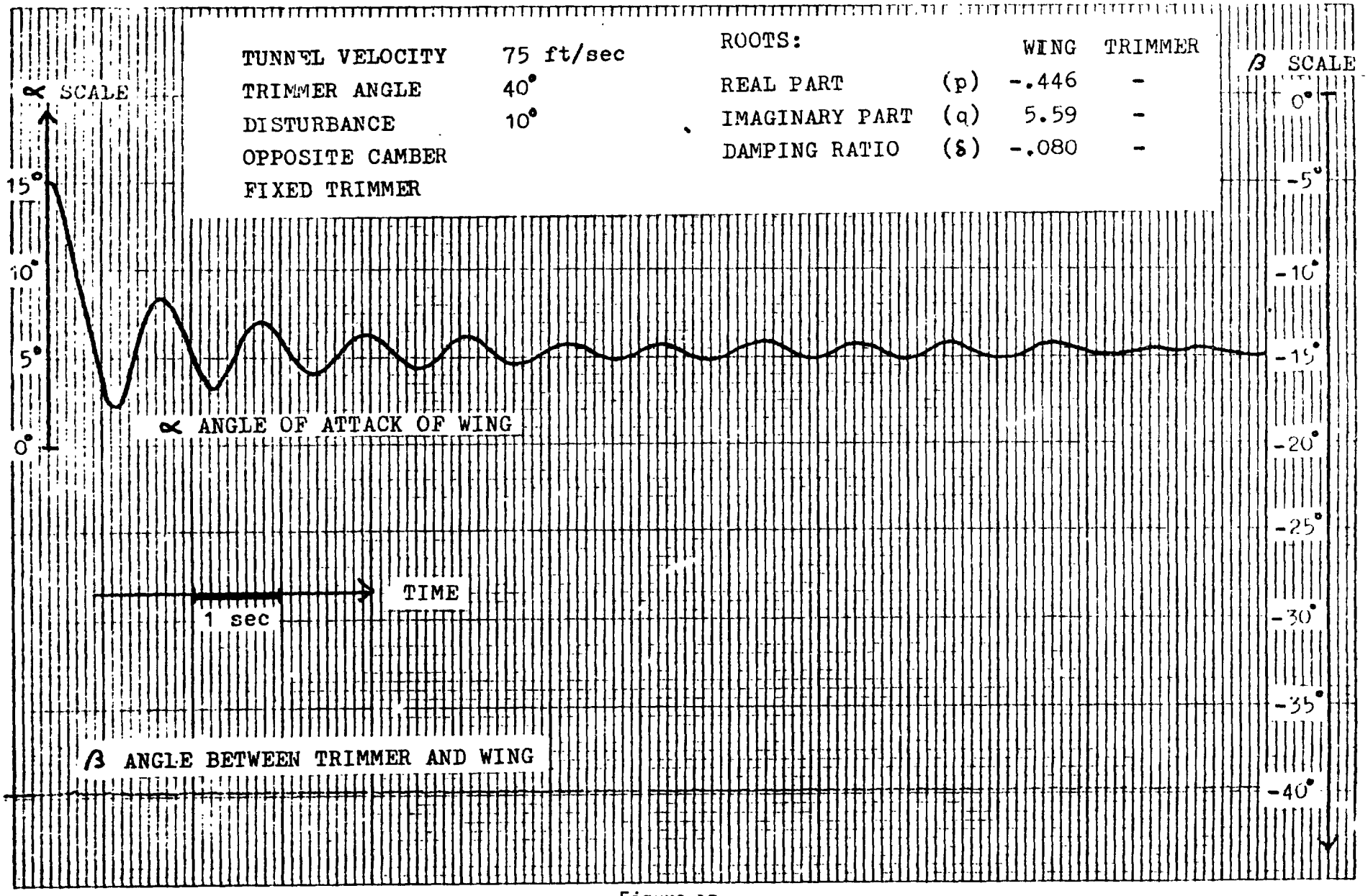

Figure 17

Time History of α with β Fixed at 40^{o} (Trimmer Stalled)

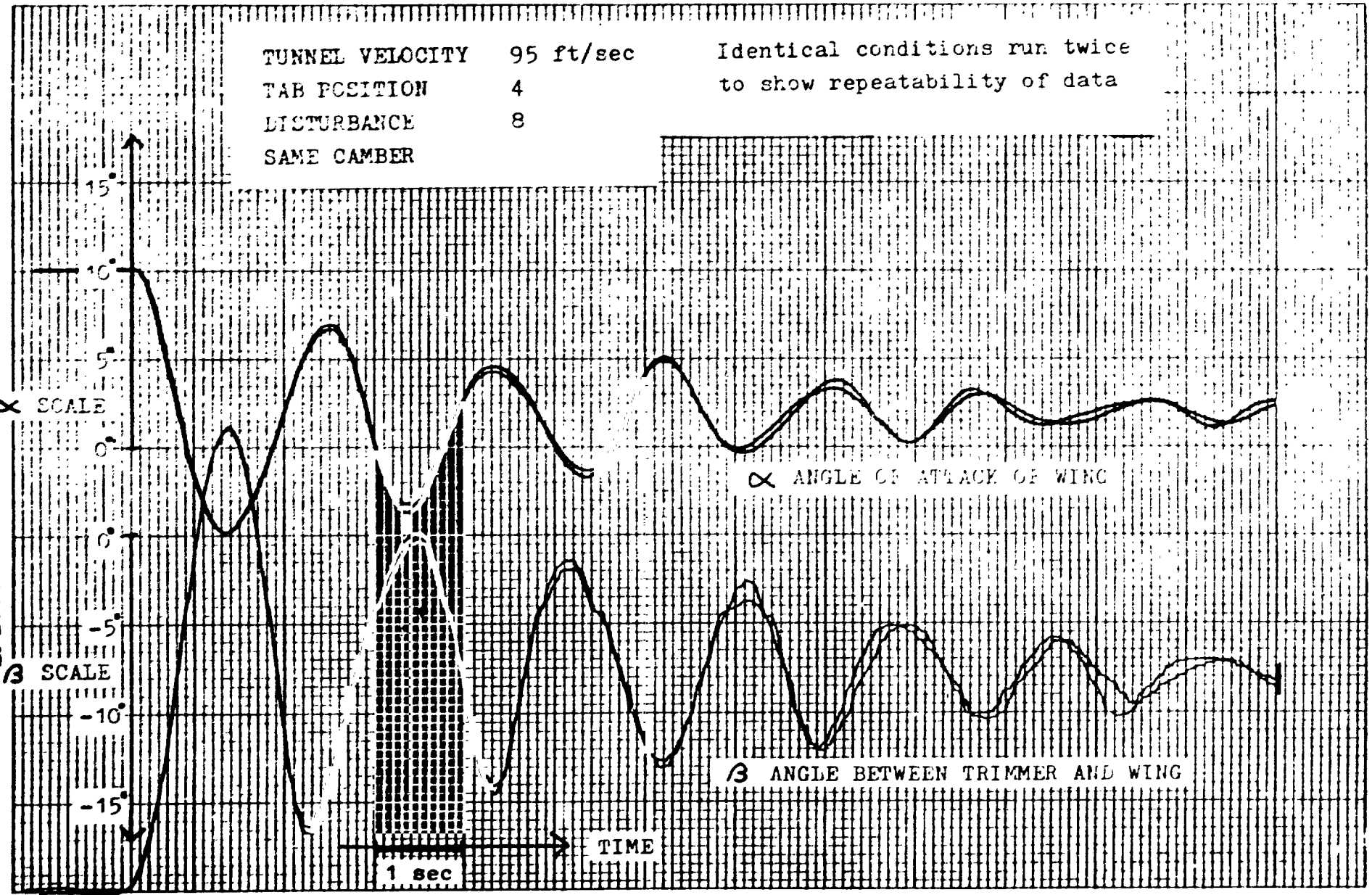

ORIGINAL PAGE IS OF POOR QUALITY

Figure 18

Time History of α and β with Two Runs Superimposed

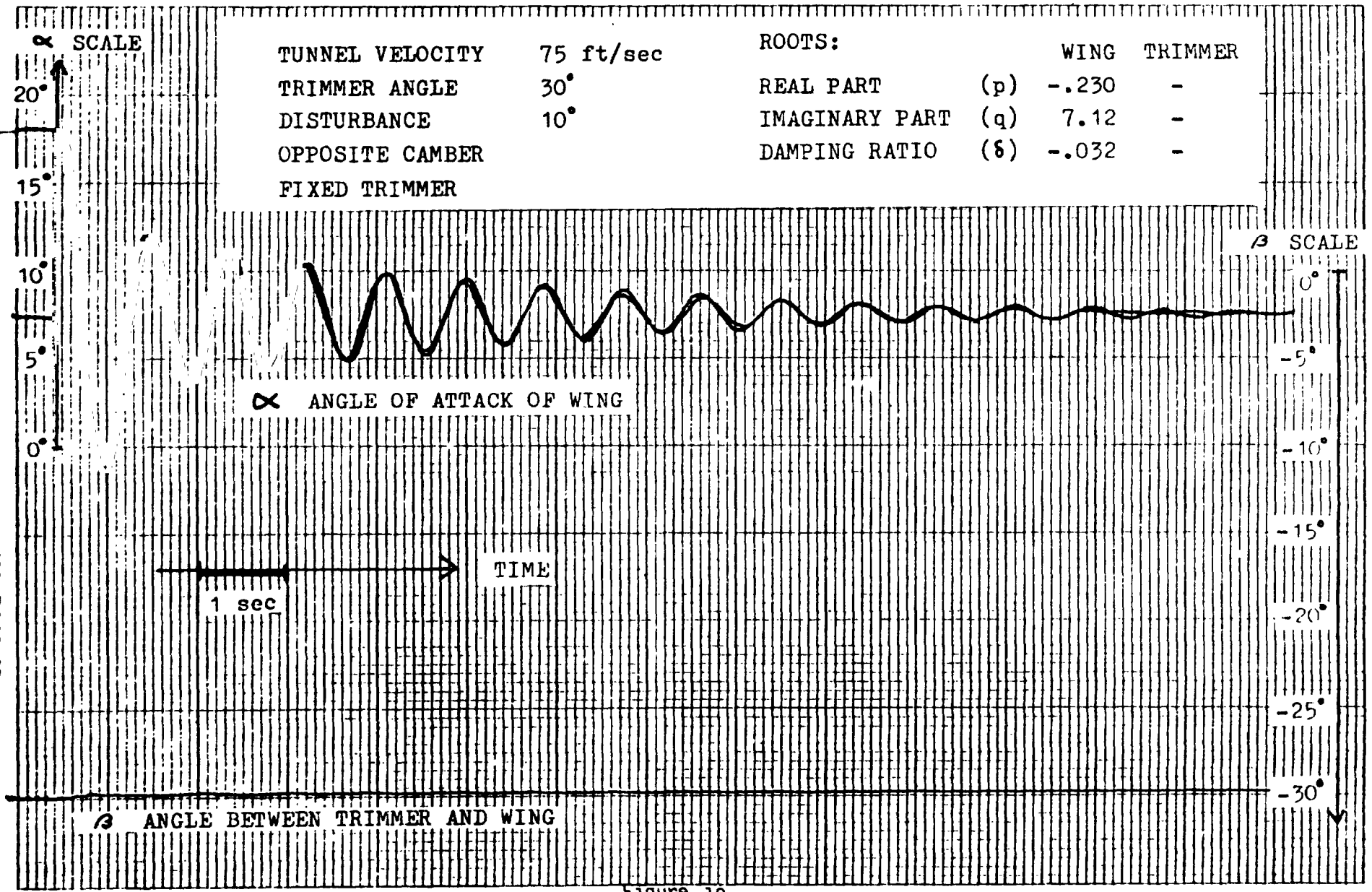

Figure 19

Time History of α with β Fixed and Two Runs Superimposed

ACKNOWLEDGEMENT

Several people assisted me on this project. I would like to express my appreciation to each. Shu Gee, of DFRC, did the preliminary investigation with radio control planes, the program definitions, and provided guidance for the free-wing/free-trimmer project.

Michael Hardaway, a student at Cal Poly, constructed a part of the model. Steve Bergevin another student at Cal Poly, helped with the moment of inertia determination and the preparation of the report.

I am especially indebted to Richard Porter of Battelle Columbus Laboratories for providing the computer predicted behavior of the free-wing/free-trimmer model. Richard also made some helpful suggestions that were used in analyzing some of the data.

The Aeronautical Engineering Department at the U.S. Naval Academy provided technician support and the use of a wind tunnel.

REFERENCES

1. Etkin, Bernard: Dynamics of Flight. New York: John Wiley & Sons, 1959.

2. Gee, Shu Wi; and Brown, Samuel R.: Flight Tests of a Radio-Controlled Airplane Model with a Free-Wing, Free Canard Configuration. WASA TM-72853, March, 1978.

3. Porter, Richard F.; and Borwn, Joe H., Jr.: Evaluation of the Gust-Alleviation Characteristics and Handling Qualities of a Free-Wing Aircraft. NASA CR-1523, July 1970.

4. Porter, Richard F.; Hall, David W.; Brown, Joe H., Jr, and Gregore Gerald M.: Analytical Study of a Free-Wing/Free-Trimmer Concept. NASA CR-2946, February 1978.

5. Porter, Richard F.; Hall, David W.; and Bergara, Rudolfo D.: Extended Analytical Study of the Free-Wing/Free-Trimmer Concept. NASA CR 3135, April 1979.

6. Porter, Richard F.; Luce, Ross G.; and Brown, Joe H., Jr.: Investigation of the Applicability of the Free-Wing Principle to Light General Aviation Aircraft. NASA CR-2046, June 1972.

7. Ho, Yu Hang, On the Dynamic Yawing of Aircraft, MS Thesis, California Polytechnic State University, November 1980.